Inorg. Chem. **2004**, *43*, 6300–6306

Unprecedented Oxo-Titanium Citrate Complex Precipitated from Aqueous Citrate Solutions, Exhibiting a Novel Bilayered Ti_8O_{10} Structural Core

Tim Kemmitt,*,† Najeh I. Al-Salim,† Graeme J. Gainsford,† Andrea Bubendorfer,† and Mark Waterland‡

Industrial Research Ltd., P.O. Box 31-310, Lower Hutt, New Zealand, and Institute of Fundamental Sciences, Massey University, Private Bag 11-222, Palmerston North, New Zealand

Received February 23, 2004

Aqueous titanium citrate solutions were prepared from the reaction of citric acid with titanium 2-propoxide in a range of molar ratios. Solutions containing two or fewer citrates per titanium resulted in the slow crystallization of an insoluble titanium oxo-citrate complex. Single-crystal X-ray analysis identified the species as $Ti_8O_{10}(citrate)_4(H_2O)_{12}\cdot 14H_2O\cdot 3HOPr^i$, crystallized in the tetragonal space group $I4_1/a$, with $a = 30.775(7)$ Å, $c = 14.528(7)$ Å, $V = 13\,759(8)$ Å^3, and $Z = 8$. The trianionic citrate ligands supply both carboxylate and alkoxide coordination and stabilize the structure using simultaneous chelating and bridging modes of attachment. The compound is a neutral species, exhibiting titanium in three contrasting environments. Laser Raman microscopy and ^{13}C CPMAS solid-state NMR data were consistent with those of the X-ray crystal structure. When exposed to air, the crystals rapidly lost water and became a powder. The dehydrated powder was noncrystalline to X-rays and insoluble, but ^{13}C NMR results demonstrated retention of the carboxylate linkages.

Introduction

Strategies to temper the sensitivity of metal alkoxides to hydrolysis include modification with appropriate ligands and/or formation of oxo-alkoxides.[1,2] Carboxylate ligands have been recognized as imparting a degree of robustness to an oxo-cluster, and many examples, generally formed from the reaction of carboxylic acids with titanium alkoxides, have been reported.[3−12] Titanium citrate species are technologically very important in producing high-tech materials, and the Pechini method[13] for producing barium titanate (BT) powders is a widely utilized citrate-based route, which results in a highly homogeneous and well-crystallized product. The method has shown its versatility with its adoption in several alternative systems for preparing well-characterized mixed-oxide nanoparticulate powders[14−18] and is now more generally referred to as the polymerized citrate route. Various chemical aspects of the route have been examined,[19−21] and recently, the structure of a titanium tricitrate dianion was

* Author to whom correspondence should be addressed. E-mail: t.kemmitt@irl.cri.nz.
† Industrial Research Ltd.
‡ Massey University.

(1) Mehrotra, R. C.; Singh, A. *Chem. Soc. Rev.* **1996**, 1−13.
(2) Hubert-Pfalzgraf, L. G. *Inorg. Chem. Commun.* **2003**, *6*, 102−120.
(3) Doeuff, S.; Dromzee, Y.; Taulelle, F.; Sanchez, C. *Inorg. Chem.* **1989**, *28*, 4439−4445.
(4) Doeuff, S.; Dromzee, Y.; Sanchez, C. *C. R. Acad. Sci.* **1989**, *308*, 1409−1412.
(5) Boyle, T. J.; Alam, T. M.; Tafoya, C. J.; Scott, B. L. *Inorg. Chem.* **1998**, *37*, 5588−5594.
(6) Alam, T. M.; Boyle, T. J.; Buchheit, C. D.; Schwartz, R. W.; Ziller, J. W. *Mater. Res. Soc. Symp. Proc.* **1994**, *346*, 35−40.
(7) Papiernik, R.; Hubert-Pfalzgraf, L. G.; Vaissermann, J.; Goncalves, M. C. H. B. *J. Chem. Soc., Dalton Trans.* **1998**, 2285−2287.
(8) Kickelbick, G.; Schubert, U. *Eur. J. Inorg. Chem.* **1998**, 159−161.
(9) Mijatovic, I.; Kickelbick, G.; Schubert, U. *Eur. J. Inorg. Chem.* **2001**, 1933−1935.
(10) Pandey, A.; Gupta, V. D.; Noth, H. *Eur. J. Inorg. Chem.* **2002**, 1351−1357.
(11) Moraru, B.; Kickelbick, G.; Schubert, U. *Eur. J. Inorg. Chem.* **2001**, 1295−1301.
(12) Boyle, T. J.; Tyner, R. P.; Alam, T. M.; Scott, B. L.; Ziller, J. W.; Potter, B. G. *J. Am. Chem. Soc.* **1999**, *121*, 12104−12112.
(13) Pechini, M. Sprague Electric Company. U.S. Patent 3,330,697, 1967.
(14) Kakihana, M.; Okubo, T.; Arima, M.; Uchiyama, O.; Yashima, M.; Yoshimura, M.; Nakamura, Y. *Chem. Mater.* **1997**, *9*, 451−456.
(15) Kakihana, M.; Okubo, T.; Arima, M.; Nakamura, Y.; Yashima, M.; Yoshimura, M. *J. Sol-Gel Sci. Technol.* **1998**, *12*, 95−109.
(16) Duran, P.; Moure, C.; Villegas, M.; Tartaj, J.; Caballero, A. C.; Fernandez, J. F. *J. Am. Ceram. Soc.* **2000**, *83*, 1029−1032.
(17) Vaqueiro, P.; Lopez-Quintela, M. A. *J. Mater. Chem.* **1998**, *8*, 161−163.
(18) Liu, W.; Farrington, G. C.; Chaput, F.; Dunn, B. *J. Electrochem. Soc.* **1996**, *143*, 879−884.
(19) Kakihana, M.; Arima, M.; Nakamura, Y.; Yashima, M.; Yoshimura, M. *Chem. Mater.* **1999**, *11*, 438−450.
(20) Tsai, J.-D.; Fang, T.-T. *J. Am. Ceram. Soc.* **1999**, *82*, 1409−1415.

10.1021/ic049760r CCC: $27.50
Published on Web 09/01/2004

determined using X-ray crystallography.[22] Single-crystal X-ray studies on anionic titanium peroxo citrate ions have also been reported.[23,24] Our interest has been in producing titanium dioxide based photocatalysts, utilizing precursors with lower citrate contents and using water as a reaction medium.[25,26] A deficit of citrate ligands encourages the formation of hydrolytic species in solution but is preferred for the formation of photocatalytic thin films.[26] Citrate complexes are also of interest from a biological viewpoint as citric acid (CA) is known to be involved in metal-ion transport and metallobiological processes.[27,28] We report here on the preparation of titanium citrate solutions, their characterization by Raman spectroscopy, and the preparation, isolation, and characterization of an octanuclear titanium oxo-citrate complex by Raman microscopy, solid-state ^{13}C CPMAS NMR, and X-ray crystallography. The neutral complex was isolated from aqueous solution and exhibits an entirely new titanium oxide core structure.

Experimental Section

General Procedures. All of the experiments and manipulations were carried out open to the atmosphere. $Ti(OPr^i)_4$ (Lancaster Synthesis) and citric acid (Panreac Chimica) were used as supplied. C and H microanalyses were carried out by the Campbell Laboratory at the University of Otago. Thermogravimetric analyses were carried out on a Rheometrics STA-1500 instrument with a heating rate of 10 °C min^{-1}.

Representative Preparations. Solution A (1:2 Ti/CA). Anhydrous citric acid (19.2 g, 0.1 mol) was dissolved in 2-propanol (100 mL) and added to a rapidly stirred solution of $Ti(OPr^i)_4$ (14.2 g, 0.05 mol) in 2-propanol (50 mL). A rapid reaction ensued, causing the whole solution to gel. All of the free solvent was removed on a rotary evaporator, leaving a fine white powder. Distilled water (40 mL) was added, and the mixture was heated to 70 °C to dissolve. Further reduction on the rotary evaporator removed most of the residual 2-propanol before the solution was diluted to 50 mL with water, resulting in approximately a 1.0 M solution (based on Ti), and left to stand at room temperature.

Solution B (1:1 Ti/CA) was prepared similarly to solution A, using $Ti(OPr^i)_4$ (28.4 g, 0.10 mol) and anhydrous citric acid (19.2 g, 0.10 mol) in anhydrous ethanol and diluting the final solution to 100 mL with distilled water to form a 1.0 M Ti solution.

Solution C (2:1 Ti/CA) was prepared similarly to solution A, using $Ti(OPr^i)_4$ (56.8 g, 0.20 mol) and anhydrous citric acid (19.2 g, 0.10 mol) and diluting the final solution to 200 mL with distilled water to form a 1.0 M Ti solution.

$Ti_8O_{10}(citrate)_4(H_2O)_{12}\cdot 14H_2O\cdot 3HOPr^i$. Crystals appearing on the walls of the flasks from solutions A−C were removed for examination and X-ray crystallographic study. Preliminary X-ray data confirmed the products were all identical. The full structural analysis described below relates to the crystals obtained from solution B. Solution C had the same Ti/CA stoichiometry as the crystalline precipitate and resulted in significantly greater precipitation of the crystalline product. Yield = 17.7 g (36.4%) based on Ti. Further precipitation of the same crystalline product continued from the mother liquor over the following 6 months. (Yields of crystals from solutions A and B were invariably much lower at <5%.) Microanalysis of the crystalline material was unreliable due to varying amounts of hydration. Removal of the crystals from the mother liquor resulted in their gradual decomposition due to the loss of water of crystallization.

Physical Measurements. FT-Raman spectroscopy was carried out on freshly prepared solutions using a Bruker IFS-55 FT-interferometer bench equipped with an FRA/106 Raman accessory and utilizing OPUS (version 4.0) software. An Nd:YAG laser with a 1064-nm excitation wavelength was used. An InGaAs diode (D424) operating at room temperature was used to detect Raman scattered photons. Incident power was 200 mW, and spectral resolution was 4 cm^{-1}. A total of 200 interferograms were collected for each sample.

Raman microscopy of the crystalline $Ti_8O_{10}(citrate)_4(H_2O)_{12}\cdot 14H_2O\cdot 3HOPr^i$ complex was carried out using a Jobin Yvon Horiba HR800 instrument. The crystals were presented under a microscope coverslip with some mother liquor to prevent dehydration and concomitant degradation.

Solid-State NMR. Samples were packed in silicon nitride rotors (7 mm o.d.), retained with Vespel end caps, and spun at 5 kHz in a Doty Scientific MAS probe. Carbon-13 NMR spectra were run at 50.3 MHz on a Varian Inova-200 spectrometer. Each 5.5-ms proton preparation pulse was followed by a 2-ms cross-polarization contact time, 30 ms of data acquisition, and a 2-s recovery delay. Signals were averaged over periods between 40 and 130 min. The chemical-shift scale was calibrated relative to the resonance of polydimethylsilane (placed at −1.96 ppm) in a separate rotor.

X-ray Crystallographic Data Collection and Refinement of Structures. Crystallographic parameters are given in Table 1. Cut blocks were mounted under a nitrogen stream on a Siemens P4 SMART diffractometer with a CCD detector. Accurate cell dimensions and orientation matrices were obtained by least-squares refinements. The data were corrected for background, Lorentz, and polarization factors and crystal decay (SAINT[29]), and an empirical absorption correction was applied (SADABS[29]). The data were collected using molybdenum radiation, λ(Mo Kα) = 0.71073 Å, with a graphite monochromator. The structures were solved by direct methods using SHELXS-90[30] and successive difference Fourier syntheses. Refinement calculations were performed using SHELXL-97.[31] All non-hydrogen atoms, except the O3W, O4W, and O7W multiple-site sets which had common isotropic parameters, were refined with anisotropic thermal parameters. Hydrogen atoms were included in calculated positions (C−H 0.99 Å) and restrained to the same occupancy and U_{iso} value 1.2 times the U_{eq} of the parent atom. Bound water (O20, O21···O25) H atoms were only included if located on a difference Fourier map and then were also restrained to O−H 0.84 Å. Hydrogen atoms located on water O atoms (O2W, O6WA, and 2-propanol O40) were restrained to O−H 1.00 Å.

(21) Fang, T.-T.; Wu, M.-S.; Tsai, J.-D. *J. Am. Ceram. Soc.* **2002**, *85*, 2984−2988.
(22) Zhou, Z.-H.; Deng, Y.-F.; Jiang, Y.-Q.; Wan, H.-L.; Ng, S.-W. *J. Chem. Soc., Dalton Trans.* **2003**, 2636−2638.
(23) Kakihana, M.; Tada, M.; Shiro, M.; Petrykin, V.; Osada, M.; Nakamura, Y. *Inorg. Chem.* **2001**, *40*, 891−894.
(24) Dakanali, M.; Kefalas, E. T.; Raptopoulou, C. P.; Terzis, A.; Voyiatsis, G.; Kyrikou, I.; Mavromoustakos, T.; Salifoglou, A. *Inorg. Chem.* **2003**, *42*, 4632−4639.
(25) Kemmitt, T.; Al-Salim, N. I.; Waterland, M.; Kennedy, V.; Markwitz, A. *Curr. Appl. Phys.* **2004**, *4*, 189−192.
(26) Kemmitt, T.; Al-Salim, N. I.; Ono, H. JSR Corporation. JP Patent No. 2000334310, 2000.
(27) Glusker, J. P. *Acc. Chem. Res.* **1980**, *13*, 345−352.
(28) Schneider, K.; Muller, A.; Krahn, E.; Hagen, W. R.; Wassink, H.; Knuttel, K.-H. *Eur. J. Biochem.* **1995**, *230*, 666−675.
(29) *SAINT* and *SADABS*; Siemens Analytical X-ray Systems, Inc.: Madison, WI, 1994.
(30) Sheldrick, G. M. *Acta Crystallogr.* **1990**, *A46*, 467−473.
(31) Sheldrick, G. M. *SHELXL-97*: *Program for the Refinement of Crystal Structures* and *CIFTAB*: *Program for Publication of Structures*; University of Gottingen: Göttingen, Germany, 1997.

Table 1. Crystallographic Parameters

formula	$C_{16.5}H_{48}O_{33.5}Ti_4$
fw	974.15
crystal system	tetragonal
space group	$I4_1/a$
T (K)	168(2)
a (Å)	30.775(7)
c (Å)	14.528(7)
Z	16
ρ (mg m^{-3})	1.881
V (Å^3)	13759(8)
μ (mm^{-1})	1.017
crystal size (mm)	0.40 × 0.32 × 0.18
θ range (deg)	2.75−26.39
reflections collected	49550
no. of unique data	6997
R_{int}	0.075
no. of observations[a]	4468
ratio min/max absorption coeff	0.791
no. of parameters	533
no. of restraints	14
P_1 (weighting parameter)[b]	0.0630
GOF on F^2	1.036
R_1[c]	0.046
wR2 (all data)	0.118
largest difference Fourier peaks, holes (e Å^{-3})	0.480, −0.444

[a] Intensities are 2.0 times their standard deviations (from counting statistics). [b] $W = 1/[\sigma^2(F_o^2) + P_1P^2]$, where $P = (F_o^2 + 2F_c^2)/3$. [c] $R_1 = \sum||F_o| - |F_c||/\sum|F_o|$; wR2 = $[\sum[w(F_o^2 - F_c^2)^2]/\sum[w(F_o^2)^2]]^{1/2}$.

There was conformational, incomplete occupancy disorder in some of the waters and, in particular, the 2-propanol molecules located around a 4-fold inversion site, modeled as follows. Waters O3W, O4W, and O7W were refined as three-site oxygen atoms (A, B, and C), with a fixed common isotropic U value [0.081(2) Å^2] and with refined occupancies (occupancy total of 2.91). Waters O5W and O6W were refined with anisotropic thermal parameters as two-site occupancies (A and B) to 0.856(9)/0.144(9) and 0.61(2)/0.39(2), respectively. Waters O1W and O2W were refined as anisotropic fully occupied sites; one hydrogen on O2W was located and refined as noted above. Three 2-propanol fragments were identified: (1) [O40 (H40O), C40, C41, C42], (2) [O43, C43A, C44, C45, C43B], and (3) [O31, C31, C32, C31B, C31C]. Atom occupancies for O40, H40O, and C41 were grouped with a final value of 0.587(9). All other atom occupancies were refined with one common final isotropic U value for fragments 1 and 2 [0.131(4) Å^2] and 3 (0.088 Å^2). On the basis of the final refined occupancies, the included solvent composition approximates to 7 H_2O molecules and 1.5 2-propanols per asymmetric unit: cell contents, $C_{264}H_{768}O_{536}Ti_{64}$. This solvent disorder region of the lattice could be successfully handled using PLATON'S SQUEEZE,[32] giving similar agreement factors; this confirmed the random nature of the atoms in this part of the lattice. The final full-model parameters and original data are presented here since they reflect some reasonable additional lattice-binding contacts. The largest residual electron-density peaks were located close to these latter atoms.

Results

Syntheses. The preparation of the aqueous titanium citrate solutions was achieved by a simple procedure reacting Ti(OPr^i)$_4$ with anhydrous citric acid in alcohol, followed by the removal of the solvent and redissolution in water. The resulting solutions were all photochromic, giving the familiar blue/black coloration typical of titania sols and gels on exposure to UV light.[33] The preparations described are representative of several preparations carried out for a range of citric acid contents.

Using ethanol in place of 2-propanol as the reaction solvent in the first step did not change the reaction pathway or product for any of the reaction ratios. The higher solubility of citric acid in ethanol made it more convenient for carrying out this step in ethanol on subsequent runs. The minor amount of disordered 2-propanol observed in the crystal structure varied slightly (see the crystallographic data in the Experimental Section) but did not fundamentally change the structure and was not exchanged by ethanol. In the reactions employing lower citric acid levels, the titanium alkoxide retained residual propoxide linkages prior to the addition of water. The hydrolysis thus liberated more 2-propanol, which was largely removed during further evaporation.

The order of the addition of reagents was observed to dramatically influence the reaction pathways. Precipitation of amorphous titania is the predominant result if water is added directly to Ti(OPr^i)$_4$. The precipitated titania can be peptized to form stable sols[24] using these citrate concentrations, but no crystalline phases have been observed. Reacting citric acid with Ti(OPr^i)$_4$ prior to hydrolysis of the alkoxide appears to limit the degree of hydrolysis and condensation. Despite this, the yield of crystalline material was still relatively poor, our best effort produced less than 40% yield based on titanium, and this could indicate that some solution-phase condensation still occurred in the synthesis solutions, even using this route. Although the crystals were first obtained from a solution equimolar in Ti and citrate (solution B), resynthesis using the correct reactant stoichiometry (solution C) produced higher yields. The precipitated crystals were insoluble once formed, suggesting that the solution species in the synthesis liquors differ from the eventual product. Some precipitation of crystals eventually occurred from all of the solutions prepared with two or fewer citrates per titanium, although the relatively small amount of fine crystals from solution A implies that the excess citrate has a stabilizing effect on the soluble titania species, reducing the rate and degree of hydrolysis, condensation, and, in turn, crystallization. As the crystals contain two Ti atoms per citrate, solutions containing higher citrate ratios than the crystals become increasingly titanium deficient as the crystals precipitate. A high citrate ratio limits the formation of oxo-species, and oxo-free titanium tricitrate complexes are reportedly stable in water.[22] We did not observe any crystallization occurring under the described conditions for solutions containing three citrates per titanium.

The nature of other solution species has not been unambiguously determined, but it is clear that in order for the Ti_8 oxo-complex to form, some hydrolytic species must be present. Carbon-13 NMR spectra of the aqueous solutions were investigated in deuterated water. The coordinated citrates appeared only as very flat, broad signals. Sharp signals corresponding to some free citric acid were also

(32) Spek, A. L. *Acta Crystallogr.* **1990**, *A46*, C-34.

(33) Matsumoto, T.; Murakami, Y.; Takasu, Y. *Chem. Lett.* **2000**, 348−349.

observed but accounted for only a few percent of the total citrate present. It is known that equilibria occur between coordinated and free citrates in the solutions of the related tricitrate complexes.[22] It is possible that more complex equilibria occur in the current system, both between citrate ligands and complexes and between soluble hydrolytic fragments and condensed oxo-species. Raman studies on the solutions broadly concur with the NMR studies in that they substantially show that all of the citrate is bound to the titanium in solutions containing only one citrate per two titanium atoms. Solutions prepared with higher proportions of citric acid contain citrates bound with a symmetry different than those of the former solution in addition to free citric acid. Attempts to identify the solution species using electrospray mass spectrometry did not conclusively identify any titanium hydrolysis products, but in the negative ion mode, the presence of some $Ti(citrate)_2^-$ was established in all of the solutions. Bearing in mind the reactant stoichiometries, we determined that other unidentified Ti-containing species must be present. We cannot entirely rule out the presence of the Ti_8 oxo-species in any of the solutions, but its low solubility makes it unlikely to be present in a high concentration. More likely, it is the presence of smaller variable-nature oxo-species which ultimately condense to form the Ti_8 framework.

The Ti_8 oxo-species can be regarded as a nanosized intermediate between smaller molecular species and larger sol particles. The octatitanium species observed is removed from the solution and does not participate in equilibria or further condensation of sol particles (Ostwald ripening) by virtue of its insolubility.

Microanalytical data on even freshly prepared crystals gave unreliable results due to differing amounts of hydration. Samples dried in vacuo at 50 °C for 6 h reproducibly retained approximately four coordinated water molecules according to elemental analysis. Anal. Calcd for $C_{24}H_{28}Ti_8O_{42}$: C, 21.0; H, 2.0. Found: C, 20.7; H, 2.0. The thermogravimetric data suggest that this approximate formulation is stable up to around 150 °C. The loss of so many coordinated aquo ligands in addition to the water of crystallization would result in a change of coordination numbers at the titanium centers, destroying the structural integrity of the complex. Despite this, the solid-state NMR data (see below) suggest that the connectivity of the citrate ligands remains largely intact.

X-ray Structure. Crystals of $[Ti_8O_{10}(C_6H_5O_7)_4(H_2O)_{12}]\cdot 14H_2O\cdot 3(HOPr^i)$ were isolated from solution B. The compound crystallizes in the tetragonal space group $I4_1/a$ (Table 1, $Z = 8$), with a space-group-imposed center of symmetry. The crystal structure consists of centrosymmetric neutral octamers (Figure 1) containing two planar Ti_4 layers, interlinked by four linear oxo-bridges (Figure 2). Selected bond distances and angles are shown in Table 2. The complexes are bound to each other by hydrogen bonds utilizing the water protons and carboxyl oxygens as acceptors and to some of the included solvent, water and 2-propanol (see Table 3).

The four independent titanium atoms have three different coordination environments. Each of the citrates is triply deprotonated, with the two unique carboxylates coordinated to three titaniums bridged by the central oxide (O15). One 6-coordinate titanium per layer (Ti4) has no citrate ligands and is coordinated purely by oxo-linkages and water

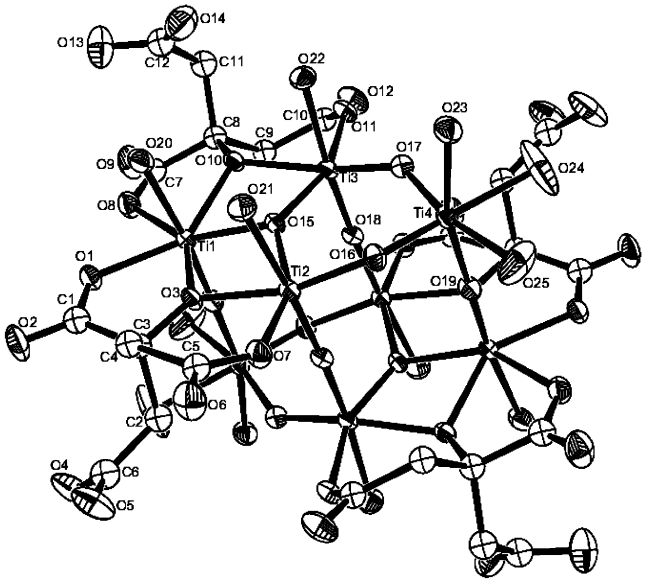

Figure 1. Molecular structure of the neutral complex $[Ti_4O_5(C_6H_5O_7)_2(H_2O)_6]_2$, showing the numbering scheme. Displacement ellipsoids are drawn at the 50% probability level. Hydrogen atoms have been excluded for clarity.[34]

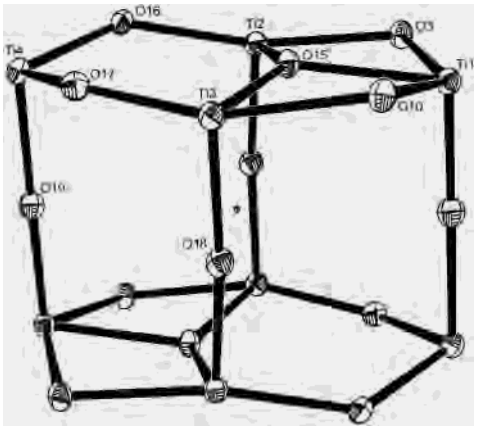

Figure 2. The "cake-plate" architecture. Ti and bridging oxygens are included, with only asymmetric unit atoms labeled. The inversion center relating other atoms is shown as the central unlabeled sphere. Displacement ellipsoids are drawn at the 30% probability level.[34]

Table 2. Selected Geometric Parameters (Å and deg)[a]

Ti1−O19^i	1.750(3)	Ti3−O17	1.812(3)
Ti1−O15	2.042(3)	Ti3−O18	1.857(2)
Ti1−O3	2.052(2)	Ti3−O15	1.887(2)
Ti1−O10	2.072(2)	Ti3−O11	2.031(3)
Ti1−O8	2.088(3)	Ti3−O10	2.060(3)
Ti1−O1	2.093(3)	Ti3−O22	2.124(3)
Ti1−O20	2.175(3)	Ti4−O16	1.785(3)
Ti2−O18^i	1.776(2)	Ti4−O17	1.832(3)
Ti2−O16	1.866(3)	Ti4−O19	1.889(3)
Ti2−O15	1.917(2)	Ti4−O24	2.113(3)
Ti2−O3	1.999(3)	Ti4−O23	2.119(3)
Ti2−O7	2.008(3)	Ti4−O25	2.132(3)
Ti2−O21	2.256(3)	Ti1^i−O19−Ti4	178.96(17)
Ti2^i−O18−Ti3	173.34(16)	O18^i−Ti2−O21	174.91(11)
O15−Ti1−O3	69.55(9)	Ti4−O16−Ti2	134.21(14)

[a] Symmetry: (i) $-x$, $1 - y$, $-z$.

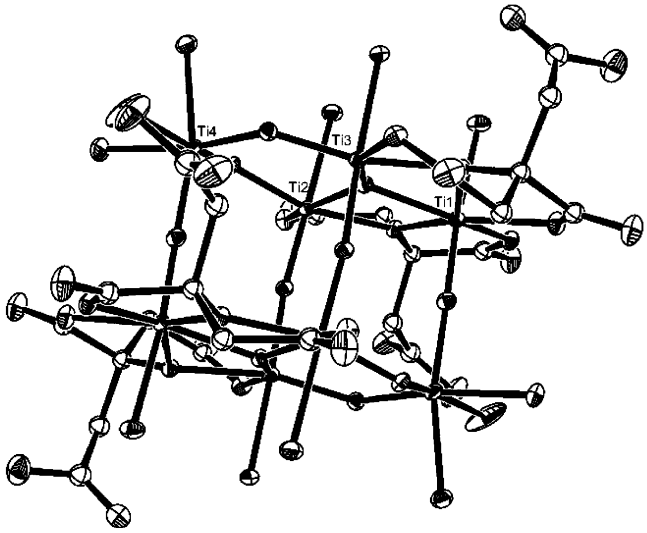

Figure 3. Alternative view of the neutral complex $[Ti_4O_5(C_6H_5O_7)_2(H_2O)_6]_2$, showing the stereochemistry due to the chirality in the coordinated citrate ligands. Displacement ellipsoids are drawn at the 30% probability level. Hydrogen atoms have been excluded for clarity.[34]

Table 3. Hydrogen-Bonding Geometries (Å and deg)[a]

D−H···A	D−H	H···A	D···A	D−H···A
O2W−H2W···O4WA^{i}	1.06(6)	2.41(6)	3.379(10)	152(5)
O4−H4O···O1W^{ii}	0.84	1.95	2.699(5)	147
O13−H13O···O1W	0.84	1.77	2.604(5)	172
O20−H201···O4WA	0.76(4)	1.89(4)	2.633(10)	166(5)
O20−H202···O5^{iii}	0.77(4)	2.24(4)	2.815(4)	132(4)
O21−H211···O5^{iii}	0.83(3)	2.19(3)	2.966(4)	156(4)
O21−H212···O6^{iii}	0.81(3)	1.94(3)	2.742(4)	175(4)
O22−H221···O14	0.82(3)	1.94(3)	2.743(4)	166(3)
O22−H222···O12i^{iv}	0.78(3)	1.95(3)	2.699(4)	162(4)
O23−H231···O12i^{iv}	0.83(3)	1.81(3)	2.640(4)	176(3)
O23−H232···O6^{iii}	0.79(4)	1.93(4)	2.712(4)	173(5)
O24−H241···O2W	0.75(5)	1.91(5)	2.654(6)	174(7)
O25−H251···O40^{iii}	0.72(5)	2.12(4)	2.778(7)	152(6)

[a] Symmetry codes: (i) $x, y, 1 + z$; (ii) $y - {}^1/_4, {}^3/_4 - x, z - {}^1/_4$; (iii) ${}^3/_4 - y, {}^1/_4 + x, {}^1/_4 + z$; (iv) $y - {}^1/_4, {}^1/_4 - x, {}^1/_4 - z$.

molecules. The two titanium atoms (Ti2 and Ti3) within each layer have distorted octahedral coordination being bound by three oxo-bridges and two oxygens from citrate trianions (terminal and μ^2-bridged), with the sixth site occupied by H_2O molecules. The other titanium atom (Ti1) is 7-coordinate, chelated by the citrate terminal oxygens (O1 and O8), the μ^2-bridging C*O$^-$ group (O3 and O10), a μ^3-oxygen (O15), a μ^2-oxygen (O19), and a water molecule (O20). The four citrates are arranged consistently with the centrosymmetric structure: two in the *R* and two in the *S* configurations (Figure 3). Thus, the neutral octameric complex has 10 oxide (O^{2-}) oxygens (O15−O19) and 12 citrato oxygens (O^{1-}) from the four bound citrates (O1,O3,O7,O8,O10,O11), a total of 32, balancing the charge of eight nominally Ti^{4+} metal ions.

The four unique titaniums are rigidly coplanar [mean deviation of 0.0028(3) Å], giving a unique configuration (from a CCDC database search[35] using Conquest;[36] for a recent summary of titanium oxo-clusters, see Boyle et al.[12]).

The bridging oxygen atoms linking the two inversion-center-related Ti atoms give a novel assemblage reminiscent of an inverse "cake-plate", with Ti−O−Ti "pillars" (Ti···Ti bond distance of 3.63 Å) (Figure 2). Both independent citrato ligands bind meridionally. As in other Ti-μ^3-O compounds, the Ti−O bond lengths vary [1.887(2)−2.042(3) Å] depending on other restraints; for example, values of 1.969(4), 1.977(4), and 1.891(4) Å are found in $[Ti_3Cl_3O_2(O_2CEt)_5]$.[37] Ti-μ^2-O bond lengths, here, vary from 1.750(3) to 2.072(2) Å, within the ranges noted before.[38] The "in-plate" Ti-μ^2-O bonds are bent [Ti−O−Ti angle of 136.5(2)°], as is commonly observed in this type of compound. The Ti−O−Ti pillars are nearly linear [176.7(2)°], which is unusual but has been observed previously in other partial hydrolysis condensates.[39,40]

There is also considerable variation in the Ti−H_2O bond lengths: 2.113(3)−2.256(3) Å. The longest value exceeds all previously reported values, with the longest being 2.183 Å in a peroxo-titanium(IV) anion.[41] An example of the more normal value for a Ti(IV)-bridged species is that found in a bis-μ^2-diaqua-methylenediphosphonato compound of 2.123 Å.[42] Interestingly, titanium atoms in distorted octahedral environments (Ti2, Ti3, and Ti4) are all slightly below the plane of their respective in-plate oxygen atoms, toward the pillar oxygens; for example, Ti4 is 0.127(2) Å below the (O24,O25,O16,O17) plane, with the latter atoms almost coplanar [mean deviation of 0.021(2) Å].

The overall composition with 7 H_2O molecules and 1.5 2-propanols per asymmetric unit is estimated from the refinement values and chemical reasonableness. Confirmation of composition by microanalysis is notoriously difficult on this type of compound[43] because the crystals decompose to a white powder with exposure to air. Crystals from solution C, with a Ti/CA ratio of 2:1 (the correct stoichiometry), were isolated for comparison. The crystals proved to be identical, giving the same octanuclear structure, similar water solvent positions, and a similar, but not identical, disorder of the 2-propanol molecules, with approximately the same 4-fold inversion site [*a* and *c* cell values were 30.706(6) and 14.606(4) Å, respectively, $V = 13\,771$ Å^3 at 158 K]. The 6989 independent reflections had similar, but poorer, internal agreement ($R = 0.076$), and the final refinement *R* was also greater than that for the initial crystal data set reported here.

Thermal analysis data are reported for the crystalline material run in 7.5% O_2 in N_2 since higher oxygen levels resulted in uncontrollable combustion during decomposition.

(34) Farrugia, L. J. ORTEP-3 for Windows. *J. Appl. Crystallogr.* **1997**, *30*, 565.
(35) Allen, F. H. *Acta Crystallogr.* **2002**, *B58*, 380−388.
(36) Bruno, I. J.; Cole, J. C.; Edgington, P. R.; Kessler, M.; Macrae, C. F.; McCabe, P.; Pearson, J.; Taylor, R. *Acta Crystallogr.* **2002**, *B58*, 389−397.
(37) Barrow, H.; Brown, D. A.; Alcock, N. W.; Errington, W.; Wallbridge, M. G. H. *J. Chem. Soc., Dalton Trans.* **1994**, 3533−3538.
(38) Kemmitt, T.; Al-Salim, N. I.; Gainsford, G. J. *Eur. J. Inorg. Chem.* **1999**, 1847−1849.
(39) Kemmitt, T.; Al-Salim, N. I.; Gainsford, G. J. *Inorg. Chem.* **2000**, *39*, 6067−6071.
(40) Weymann-Schildknetch, S.; Henry, M. *J. Chem. Soc., Dalton Trans.* **2001**, 2425−2429.
(41) Schwarzenbach, D. *Inorg. Chem.* **1970**, *9*, 2391.
(42) Serre, C.; Ferey, G. *Inorg. Chem.* **1999**, *38*, 5370−5373.
(43) Kemmitt, T.; Gainsford, G. J.; Al-Salim, N. I. *Aust. J. Chem.* **2002**, *55*, 513−517.

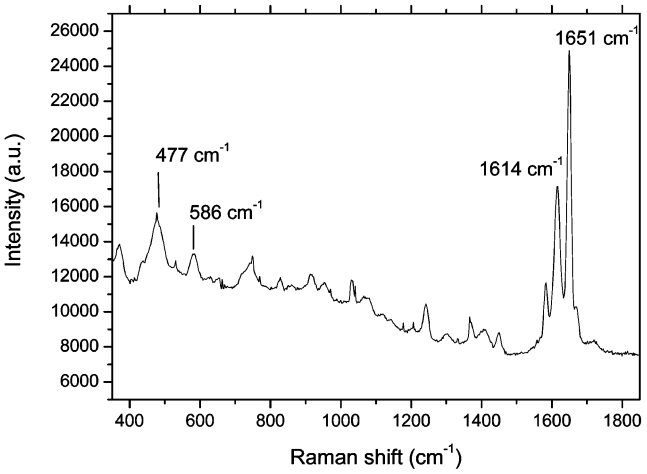

Figure 4. Raman microscopic spectrum of crystalline $Ti_8O_{10}(citrate)_4(H_2O)_{12}\cdot 14H_2O\cdot 3HOPr^i$.

Three major weight-loss regions were apparent. The lower temperature region, from ambient up to around 150 °C, is further split into approximately three events. The first corresponds to the loss of 14 H_2O and three 2-PrOH molecules (calcd 22.18%). The second, beginning around 80 °C, corresponds to a further loss of 8 H_2O molecules (calcd 7.40%), with the final 4 H_2O molecules being lost above 150 °C (calcd 3.7%). The total observed weight loss in this region is 34.7%, compared with the expected 33.3%. The processes in this region are not entirely sequential; thus, it is difficult to accurately separate the events into entirely accurate weight-loss steps. However, this is consistent with the proposed structure and also broadly agrees with the formulation of the vacuum-dried sample, which apparently retains four coordinated aquo ligands. A second endothermic event began around 250 °C, consistent with the loss or decomposition of most of the citrate ligands (23.2% weight loss), and finally, a highly exothermic combustion of the residual organic content began at 480 and ended at 580 °C under the described conditions (8.9% weight loss). Total weight loss from 30.217 to 10.002 mg was 66.90%. When a total conversion to TiO_2 is assumed, the theoretical weight loss from the crystalline $Ti_8O_{10}(citrate)_4(H_2O)_{12}\cdot 14H_2O\cdot 3HOPr^i$ should be 67.18%.

Raman Microscopy. Individual crystals of the complex were investigated using laser Raman microscopy. The spectrum (Figure 4) is characterized by sharp, strong carboxylate vibrations between 1580 and 1660 cm^{-1}, a broad signal with a Raman shift centered at 477 cm^{-1} attributed to the ν(Ti−O) modes of the oxo core, and a weaker shift at 586 cm^{-1} associated with the ν(Ti−O) modes of the coordinated citrates. By contrast, the Raman spectra of the related dimeric[24] and tetrameric[23] titanium citrate anions are dominated by vibrations associated with the peroxo group, with relatively weaker signals in the Ti−O and carboxylate regions.

Laser Raman spectroscopy was carried out on aqueous titanium citrate solutions to try to determine the nature of the species in solution. Samples were freshly prepared according to the synthesis methods described in the Experimental Section prior to any significant crystallization of the oxo-citrate complex. Three spectra from solutions having

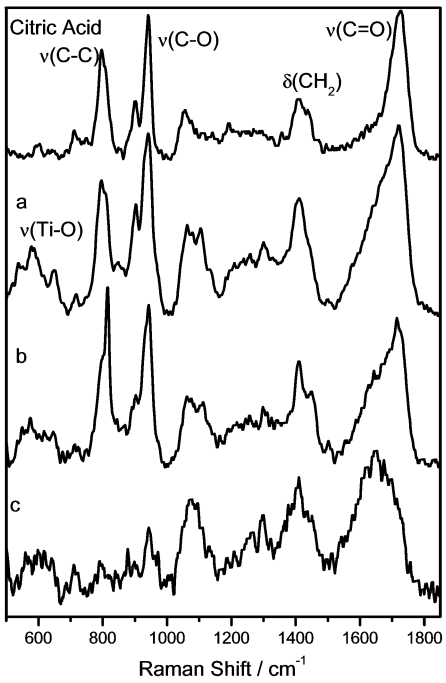

Figure 5. Laser Raman spectra of Ti/citrate solutions containing (a) 1:2, (b) 1:1, and (c) 2:1 titanium/citrate ratios.

citric acid stoichiometries of 2, 1, and 0.5 per titanium atom are shown in Figure 5a−c, respectively, together with a spectrum obtained from an aqueous citric acid solution for comparison. These can also be compared with those of the study on BaTi citrates,[19] which show some similar features.

Tentative assignments in the spectrum of citric acid have been made following Tarakeshwar.[44] The citric acid bands are present both in spectrum 5a and in spectrum 5b, but these bands are reduced, split, or feature extra shoulders consistent with the presence of chelated citrate. For example, the strong bands attributable to the ν(C═O) modes at 1728 cm^{-1} broaden to a shoulder around 1640−1650 cm^{-1}, the weaker band at 1057 cm^{-1} splits to exhibit an extra feature at 1110 cm^{-1}, and the strong band at 797 cm^{-1} shrinks and is partially displaced by a new strong band at 816 cm^{-1}. New bands at 538, 580, and 650 cm^{-1} are characteristic of the ν(Ti−O) modes associated with coordinated citrate and appear most strongly in the 2:1 citrate/Ti spectrum (Figure 5a).

The Raman spectrum of the 1:2 citrate/Ti solution (Figure 5c) is qualitatively different. Only a very minor amount of free citric acid is detectable. The new and shifted bands in spectra 5a and 5b are not present, except for the strong, broad bands associated with the ν(Ti−O) modes of coordinated citrate at around 1623 cm^{-1} and the weaker bands at 1263 and 1300 cm^{-1}. The band at 1057 cm^{-1} is shifted to 1079 cm^{-1}.

Much superior resolution is observed in the Raman spectra of the crystals where many more weaker bands can be identified. A number of bands appear in similar spectral regions to the solutions, but it is not possible to determine whether any of the solutions contain core species similar to

(44) Tarakeshwar, P.; Manogaran, S. *Spectrochim. Acta* **1994**, *50A*, 2327−2333.

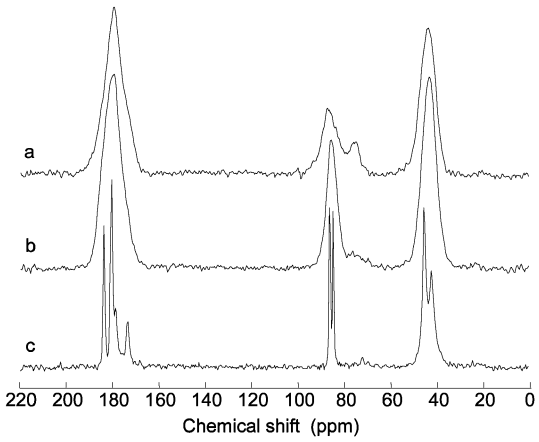

Figure 6. Solid-state ^{13}C CPMAS NMR spectra of (a) noncrystalline material produced by the removal of solvent from a Ti/citrate solution containing 1:2 citrate/titanium, (b) powder resulting from the dehydration of a crystalline titanium oxo-citrate complex, and (c) crystalline complex $Ti_8O_{10}(citrate)_4(H_2O)_{12}\cdot 14H_2O\cdot 3HOPr^i$.

those of the crystals. Without doing an ab initio calculation on the structure, it is difficult to provide a more definitive assignment for the bands.

Solid-State ^{13}C CPMAS NMR. In addition to examining the crystalline material, a sample of solution C, containing the same Ti/citrate stoichiometry as the crystals, was evaporated and dried in a oven at 60 °C overnight to form an amorphous glassy solid. The spectrum of this material (Figure 6a) shows very broad peaks, consistent with citrates existing in many environments in an amorphous solid. In comparing this spectrum with that of the crystalline solid, we observe that the citrate connectivities differ from the insoluble crystalline material. In particular, the main tertiary alkoxide carbon signal at 87 ppm appears with an additional smaller (quarter intensity) signal at 75 ppm, consistent with the hydroxyl group being only partially deprotonated. The spectrum obtained from a sample of the crystals dried in a oven at 60 °C overnight (Figure 6b) has a slightly sharper deprotonated alkoxide signal at 85.7 ppm and is accompanied by a much weaker shoulder (∼75 ppm), consistent with the presence of only a minor amount of citrate hydroxyl. The difference between these two spectra underlines the difference between the citrate connectivity in the (dehydrated) crystals and the (dehydrated) solution. Had the same species been present as the major constituent in solution as in the crystals, it is likely that the ^{13}C NMR spectra of both dehydrated samples would have been more congruent.

The spectrum obtained from a sample of freshly prepared crystalline material is shown in Figure 6c. This exhibits a clean spectrum with well-defined signals entirely consistent with the X-ray crystal structure. The four citrates bound in this molecule are arranged similarly, each binding unsymmetrically through two of the three available carboxylates and the hydroxyl group imposing chirality on the central CH group. The two citrates associated with titaniums 1−3 (Figure 3) have the same handedness, which is necessarily opposite to the other two citrates and are related by a crystallographic center of inversion. Each is, thus, a meso pair, with the dangling CH_2COOH arranged axially and equatorially with respect to the plane defined by the set of titaniums 1−4. This results in the splitting of some of the ^{13}C NMR signals, illustrated by the appearance of two lines for the unbound carboxylate (178.8 and 173.4 ppm). The two bound carboxylate groups exhibit one signal each (183.6 and 180.2 ppm). The central CHO signal is split into two narrow lines at 86.1 and 84.6 ppm, both consistent with the hydroxyl being deprotonated and bound to the metal center. The CH_2 molecules adjacent to the bound and dangling carboxylate signals exhibit separate signals, with presumably the CH_2 on the dangling carboxylate being broader due to some motional averaging, preventing resolution of the splitting.

Conclusions

Accessing titanium citrate solutions via the anhydrous reaction of citric acid with $Ti(OPr^i)_4$ was successful in avoiding the uncontrolled hydrolysis and precipitation of hydrous titania. Aqueous titanium citrate solutions containing two or fewer citrates per titanium atom were found to not form stable complexes in solution; however, partial hydrolysis fragments condense to form a highly hydrated, insoluble Ti_8 oxo-complex. Solid-state ^{13}C NMR and Raman microscopy data are consistent with the X-ray crystal structure.

Acknowledgment. This work was funded by the New Zealand Foundation for Research in Science and Technology (Contract CO8X0212). We thank the staff of the University of Canterbury's Crystallography Laboratory for the X-ray data collection, Dr. R. Newman for assistance with the ^{13}C CPMAS NMR spectra, the University of Otago's Campbell Laboratory for microanalytical data, and the University of Waikato for electrospray mass spectral data.

Supporting Information Available: X-ray data and details of refinement procedures (CIF). This material is available free of charge via the Internet at http://pubs.acs.org.

IC049760R